Anal. Bioanal. Electrochem., Vol. 9, No. 8, 2017, 1029-1043

Analytical & Bioanalytical Electrochemistry

Full Paper

Simultaneous Voltammetric Determination of Uric Acid and Tryptophan by Modified Graphite Paste Electrode with Ferrocyanide Ions-doped Nano Resin Lewatit FO_{36} as a New Redox Probe

Somayeh Rigi Ladiz and Meissam Noroozifar*

Analytical Research Laboratory, Department of Chemistry, University of Sistan and Baluchestan, P.O. Box 98135-674, Zahedan, Iran

*Corresponding Author, Tel.: +985433416464; Fax: +985433416888
E-Mail: mnoroozifar@chem.usb.ac.ir

Received: 1 May 2017 / Received in revised form: 19 October 2017 / Accepted: 31 October 2017 / Published online: 31 December 2017

Abstract- A novel, selective and sensitive modified graphite paste electrode (GPE) containing ferrocyanide anionic complexs (FCN) doped-Nano resin Lewatit FO36 (NRL) was designed for simultaneous determination of Uric acid (UA) and Tryptophan (Trp). The above modified electrode was investigated by various techniques such as transmission electron microscopy, Fourier transform infrared spectroscopy, cyclic voltammetry (CV), and electrochemical impedance spectroscopy (EIS). The electrochemical behaviour of the UA and Trp was investigated at FCNNRL/GPE by CV, differential pulse voltammetry and Chronoamperometry techniques in pH 3. Under the optimum conditions, the calibration curves were linear in the ranges of 0.4-175.2 µM and 0.5-173 µM with detection limits 10 and 30 nM, for UA and Trp, respectively. The above sensor can be successfully was used for the determination of UA and Trp with high sensitivity and accuracy in real samples.

Keywords- Redox probe, Ferrocyanide anionic complexs doped- Nano resin Lewatit FO_{36}, Simultaneous determination, Uric acid, Tryptophan

1. INTRODUCTION

Uric acid (UA) is a major product of urine metabolism and its abnormal levels in blood can lead to several diseases like gout, hyperuricemia, leukemia, pneumonia and Lesch–Nyhan

syndrome [1]. Hence, the determination of UA in blood and urine is highly important. Tryptophan (Trp) is an essential amino acid for the production of hormones, neurotransmitters and other biomolecules in human diet and the abnormal concentrations of Trp can lead to hepatic disease [2]. So, it is very important to develop a simple, efficient and rapid analytical technique for determination of biological molecules such as UA and Trp, because as mentioned, many of diseases are related with their concentrations into biological fluids. Determination of UA and Trp have been done by following different methods: high performance liquid chromatography [3-6], capillary electrophoresis [7-9] and spectrophotometry [10,11] as well as electrochemical techniques [12-17]. The mentioned above methods except latter are performed with the high costs and time consuming. The most of above methods, measurement of analytes is started after of carried out extraction or pre-treatment. The electrochemical techniques in the comparison with these above measurement methods have the benefits such as fast response, high sensitivity, very well accuracy, excellent selectivity, cheap and simplicity instrument, low cost and less time consuming [18-20].

The Nano resin Lewatit FO_{36} (NRL) (Lewatit polymer resin (FO_{36}) based iron oxide nanoparticles doped) is based on a polymeric, macroporous, anion exchange resin which is doped with a nano-scaled film of iron oxide involving hydroxy-groups [21]. Iron hydroxides (FeOOH) can act as the anion exchange surfaces for a variety of anions which given the large surface area [21]. The Ferrocyanide anionic complex can be exchanged with hydroxy-groups from the NRL surface and the product can be used as modifier in the paste electrodes (PE). The great surface area and optimised pore structure of NRL act as absorbent these electroactive biomolecules to the NRL/PE surface. In this study, a simple and rapid analytical technique which combines the considerable properties of NRL doped with ferrocyanide anionic complex (FCN) with physical and chemical properties of graphite paste electrodes (GPE), such as low background currents, high conductivity, hydrophobicity, variable potential window, easy preparation, modification and surface regeneration and low cost [22] was used for measurement of biological molecules UA and Trp. The FCNNRL/GPE makes high sensitivity and selectivity for the determination of UA and Trp in chloroacetic acid buffer solution (CABS) 0.1 M at pH 3.0. Finally, above sensor has been successfully applied for measurement of these mentioned molecules in real samples.

2. EXPERIMENTAL

2.1. Reagents and materials

Iron oxide nanoparticles resin Lewatit (FO_{36}) was prepared from Germanic Company (Lanxess Company). The potassium hexacyanoferrate (II) and (III), viscosity paraffin oil (density=0.88 g ml^{-1}), graphite powder, Tryptophan (Trp), Uric acid (UA) and NaOH were

purchased from Merck Company. The solutions 1.0×10^{-2} M of UA and Trp were prepared by dissolving in doubly distilled water (DDW). The above solutions were daily prepared. Chloroacetic acid (CA) and acetic acid (AA) were purchased from May & Bayker and Merck Companies, respectively. The buffers with different *p*Hs were prepared with 0.1 M NaOH solution and CA and AA solutions. The CA and AA buffer solutions denoted as CABS and AABS, respectively. The CA (pK_a=2.87) was used for pH 2-3.8 and the AA (pK_a=4.76) was used for pH 3.8-5.8 were used. All solutions were prepared with double distilled water (DDW). The serum and urine real samples were obtained from the Omid Clinical Laboratory (Zahedan, Iran) and passed through a filter with suitable porosity. The de-oxygenations from electrolyte solutions were performed with high-purity nitrogen bubbling before each voltammetric measurements. The nitrogen atmosphere at room temperature is used for performance all electrochemical experiments.

2.2. Instrumentation

Cyclic voltammetric (CV), differential pulse voltammetric (DPV) and chronoamperometric (CHA) experiments were carried out with a SAMA500 Electroanalyser (SAMA Research Center, Isfahan, Iran). The experiments were performed using a conventional three-electrode cell included, the modified graphite paste electrode(GPE) with 5.0 mm diameter as the working electrode, a platinum electrode as the auxiliary, and a saturated calomel electrode (SCE) was used as the reference electrode. Electrochemical impedance spectroscopy (ESI) was performed with an Autolab PGSTAT 128N (EcoChemie, Netherlands) potentiostat/galvanostat controlled by NOVA 1.11 software. Electrochemical impedance measurements were performed in 5 mM $[Fe(CN)_6]^{3-/4-}$ prepared in 0.1 M KCl. EIS was performed over a frequency range of 0.1 Hz to 100 kHz with 0.02 V amplitude (rms). Electrolyte solutions were cleared with high-purity nitrogen before electrochemical experiments. A Metrohm 632 pH-meter with a Metrohm double junction glass electrode was used for monitoring any pH adjustment. The nanoparticles size of FCNINRL was obtained using a Zeiss CEM 902A transmission electron microscopy (TEM). The infrared spectrum of the FCNNRL/GPE and NRL/GPE were taken by a Nicolet 5DX FT-IR spectrometer using KBr pellets.

2.3. Preparation of working electrode

For Preparation of NRL doped with FCN, 0.1 gr of the NRL was mixed with 10 mL of $[Fe(CN)_6]^{3-/4-}$ solution (1.0×10^{-3} M, 25 ◦C) and stirred for 90 min at 450 rpm. The ferrocyanide complexes were exchanged with hydroxy-groups of iron ions (Fe^{3+} and Fe^{2+}) on the inner surfaces of the NRL [21] and the we suggested that the Prussian Blue was formed onto of NRL. In fact, the Prussian Blue is ferric ferrocyanide ($Fe_4^{III}[Fe^{II}(CN)_6]_3$) with iron(III) atom coordinated to nitrogen and iron(II) atom coordinated to graphite [23]. It is

know that the Prussian Blue can be synthesized chemically by mixing of ferric (ferrous) and hexacyanoferrate ions solution with different oxidation state of iron atoms: either Fe^{3+} + $[Fe^{II}(CN)_6]^{4-}$ or Fe^{2+} + $[Fe^{III}(CN)_6]^{3-}$. The result product denoted as FCNNRL. The obtained FCNNRL washed with double distilled water and then dried in air. The GPE was prepared by hand-mixing the graphite powder with paraffin oil (65:35 w/w) in a mortar. For preparation of FCNNRL/GPE and NRL/GPE, a mixture of 3.0% (w/w) FCNNRL or NRL with graphite powder was blended then the above resulting mixture and paraffin was mixed with a mortar. The obtained paste was packed into the end of a polypropylene tube. For implement electrical contact a copper wire was inserted into the above tube.

3. RESULTS AND DISCUSIION

3.1. Characterization of the FCNNRL/GPE

Figure 1(a) shows transmission electron microscopy (TEM) image of FCNNRL/GPE. The FCNNRL sizes were estimated <100 nm. Supporting evidence for this modified electrode found by the comparison Fourier transform infrared spectroscopy of FCNNRL with infrared spectroscopy of NRL. Figure 1(b) was shown the FT-IR spectrums of NRL and FCNNRL which the FT-IR spectra of FCN-NRL displays a peak at 2105.63 cm^{-1} related to cyano groups of $[Fe(CN)_6]^{3-/4-}$ [24] and also peak at 2044.73 cm^{-1}, which was attributed to cyano groups stretching vibration. These results display that ferrocyanide anionic complex was exchanged with hydroxy groups within nanoparticles on the surface of NRL.

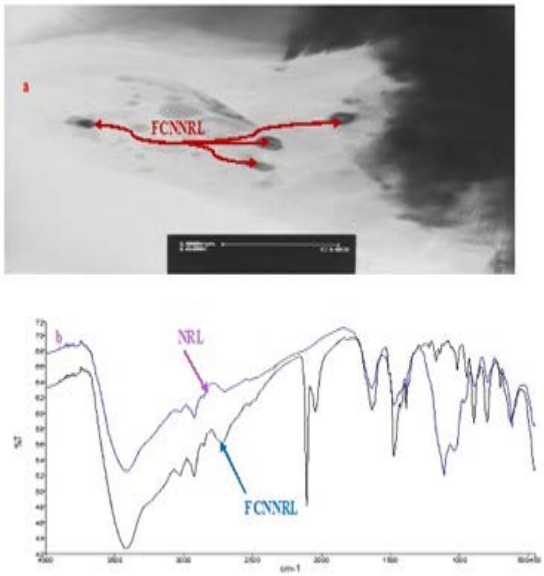

Fig. 1. (a) TEM image of FCNNRL/GPE and (b) FT-IR spectrum image of NRL/GPE and FT-IR spectrum image of FCNNRL/GPE in KBr pellet

3.2. Electrochemical impedance spectroscopy

The charge transfer processes in the different electrodes were studied by monitoring charge transfer resistance (R_{ct}) at the electrode and electrolyte interface. The value of the R_{CT} depends on the dielectric and insulating features at the electrode/electrolyte interface. The interfacial information of FCNNRL/GPE, NRL/GPE and GPE was characterized by electrochemical impedance spectroscopy (EIS). Figure 2(a) displays the EIS spectrum of the GPE, NRL/GPE and FCNNRL/GPE modified electrodes in KCl solution (0.1 M) containing the $[Fe(CN)_6]^{3-/4-}$ solution (5 mM) (1:1) with the frequencies swept from 10^5 to 10^{-1} Hz. the Nyquist plots can be analyzed by Randles equivalent circuit which shows in inset of Figure 2(a). The electron transfer resistance (R_{ct}) value which were 17.9, 5.0 and 2.7 kΩ for GPE, NRL/GPE and FCNNRL/GPE, respectively. It was observed that the R_{ct} of the FCNNRL/GPE modified electrode is lower than that of the GPE, NRL/GPE electrodes. The results show that the FCN in FCNNRL/GPE decreases the resistance of the electrode and holds high electron transfer efficiency, while the R_{ct} of the GPE and NRL/GPE electrodes increases over that of the FCNNRL/GPE modified electrode. This increase in R_{CT} is attributed to the fact that GPE and NRL/GPE are poor electrical conductors at low frequencies and cause hindrance to electron transfer. These results also indicate binding of FCN onto the NRL of FCNNRL/GPE electrode.

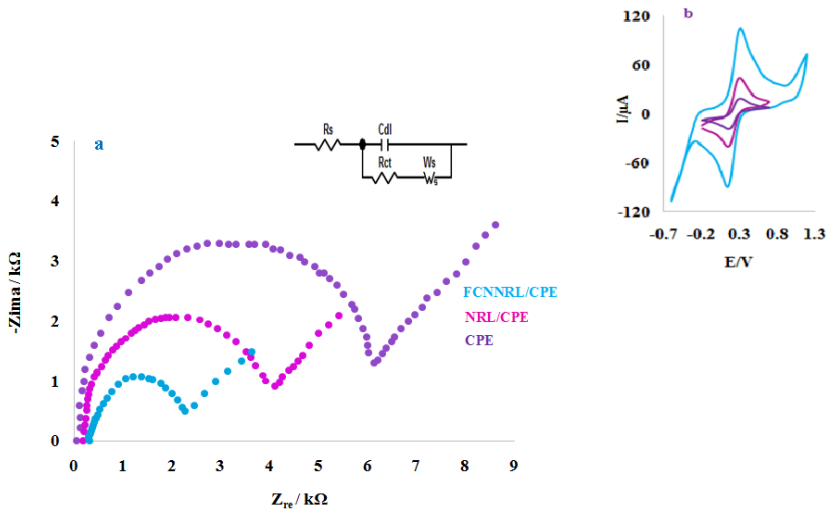

Fig. 2. (a) the EIS spectrum of the FCNNRL/GPE, NRL/GPE and GPE in KCl solution (0.1 M) containing the $[Fe(CN)_6]^{3-/4-}$ solution (1.0×10^{-3} M) with the frequencies swept from 10^4 to 10^{-1} Hz.3; (b) The cyclic voltammograms of FCNNRL/GPE, NRL/GPE and GPE in the above mentioned solution

Figure 2(b) displayed the cyclic voltammograms of FCNNRL/GPE, NRL/GPE and GPE in the above mentioned solution. Based on Figure 2(b), the anodic and cathodic peak currents

of FCNNRL/GPE is more than NRL/GPE and GPE which was in good agreement with the results obtained from of the EIS study.

3.3. The electrochemical characterization of FCNNRL/GPE

The electrochemical behaviour of NRL/GPE and FCNNRL/GPE were studied by cyclic voltammetry over a potential range from – 0.5 to 1 V in the CAB solution 0.1 M at pH 3.0. The results were shown in Figure 3(a). Based on this figure, there is not any voltammetric response for the NRL/GPE but for the FCNNRL/GPE there is one well defined reversible voltammetric response corresponding to the $[Fe(CN)_6]^{3-/4-}$ redox system. Figure 3b shows the cyclic voltammograms of FCNNRL/GPE at the different scan rates (10-130 mV/s).

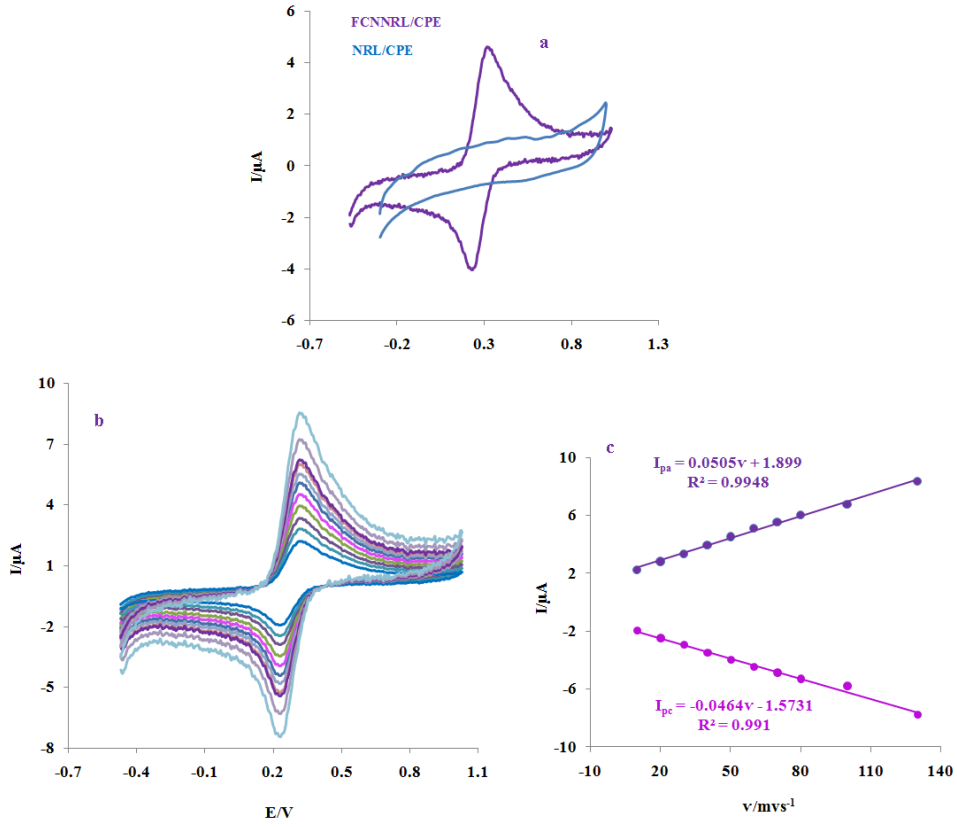

Fig. 3. (a) Cyclic voltammograms of modified paste electrodes FCNNRL/GPE and NRL/GPE in CABS (0.1 M) at pH 5.0. Scan rate: 50 mV/s; (b) Cyclic voltammograms of FCNNRL modified GPE in 0.1 mol L^{-1} CABS (pH 3.0) at various scan rates (of inner to outer curve): 10, 20, 30, 40, 50, 60, 70, 80, 100, 130 mV s^{-1}; (c) Plots of anodic and cathodic peak currents of FCNNRL/GPE *vs*. scan rates

A couple of reduction and oxidation peaks at 0.229 and 0.285 V with peak potential separation ΔE_P=0.056 V (or 56 mV) was acquired that is smaller than the 59/*n* mV (with n=1 for number of electrons for $[Fe(CN)_6]^{3-/4-}$redox system) expected for a reversible system.

Figure 3c displays a linear variation between current and scan rate with correlation coefficient (R^2) o.995 which showing surface-controlled electrode processes. These behaviours are coinciding with diffusionless system and a reversible process. A proximate amount of the electroactive species can be calculated by Sharp *et al*. method [25] for FCNNRL/GPE. Therefore the peak current is related to the surface coverage (Γ) following Eq. (1);

$$I_P = \frac{n^2 F^2 A \Gamma \nu}{4RT} \quad (1)$$

where n represents the number of electrons involved in the reaction (n=1), A is the surface area of the electrode (0.2 cm^2), I_P is the peak current, Γ represents the surface electroactive species concentration (mol cm^{-2}), F is Faraday's constant (96485 C mol^{-1}), R is gas constant (8.314 J mol^{-1} K^{-1}), T is the temperature (298 K) and ν is the scan rate. From the slope 0.05 (Figure 3c) of anodic peak currents versus can rate, the surface electroactive species concentration (Γ) of FeCN in FCNNRL /GPE is estimated to be about 2.69×10^{-10} mol cm^{-2}.

3.4. The effective electroactive surface area study

The active microscopic surface areas of GPE, NRL/GPE and FCNNRL/GPE were investigated by using Cyclic voltammetry (CV) technique at various scan rates in 1.0 mM $[Fe(CN)_6]^{3-/4-}$ and 0.1 M KCl solution. As shown in Figure 4, the oxidation and reduction peak currents of $[Fe(CN)_6]^{3-/4-}$ redox couple increased with increasing the scan rates. Figure 4(d) was shown a linear relationship between peak current and $\nu^{1/2}$ for GPE, INRL/GPE and FCNINRL/GPE. These results can be predicted by the Randles– Sevcik equation [21,22];

$$I_{pa} = 0.4463 A C_o \left(\frac{F^3}{RT}\right)^{1/2} n^{3/2} {D_R}^{1/2} \nu^{1/2} \quad (3)$$

where I_{pa} is anodic peak current of electroactive species, A is the electrode active surface area (cm^2), C_o is the concentration of analyte (mol. Cm^{-3}), F is Faraday's constant (96,485 C. mol^{-1}), R is the universal gas constant (8.314 J. mol^{-1} .K^{-1}), T is the temperature (298 K), n represents the number of transferred electrons, D_R is the diffusion coefficient of analyte ($cm^2.s^{-1}$) and ν is the scan rate (V. s^{-1}). For 1.0 mM $[Fe(CN)_6]^{3-/4-}$ solution in 0.1 M KCl as supporting electrolyte, n=1 and $D_R=7.60\times10^{-6}$ cm^2. s^{-1} [21,22]. Therefore, from the slopes obtained of the plots of I *vs.* $\nu^{1/2}$ relation at various scan rates, the active microscopic surface areas of GPE, NRL/GPE and FCNNRL/GPE calculated to be 0.117 cm^2, 0.324 cm^2 and 0.769 cm^2, respectively, which indicates that the presence of NRL and FCN can be increased the effective microscopic surface areas of the modified electrodes.

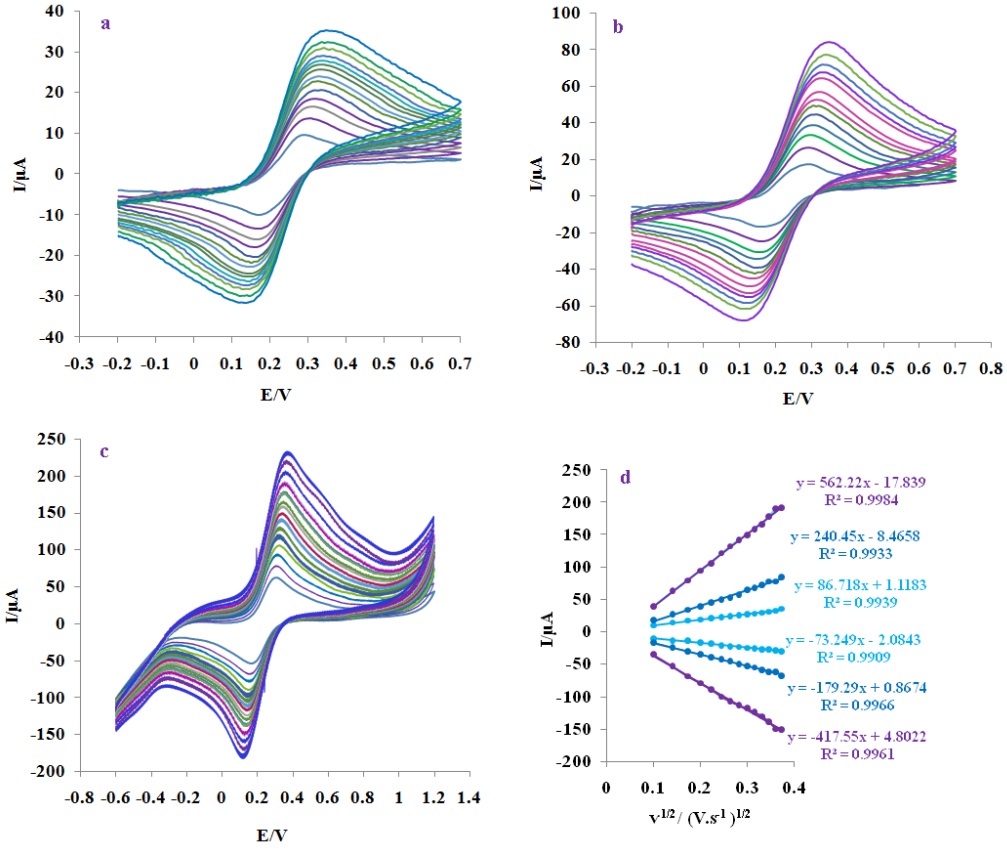

Fig. 4. Cyclic voltammograms of (a) GPE, (b) NRL/GPE and (c) FCNNRL/GPE in the presence of $[Fe(CN)_6]^{3-/4-}$ (1.0 mM) in 0.1 M KCl, at various scan rates (from inner to outer curve): 10, 20, 30, 40, 50, 60, 70, 80, 90, 100, 110, 120, 130, 140 and 150 mV s^{-1}. (d) Plots of anodic and cathodic peak currents for each electrode *vs*. $\upsilon^{1/2}$

3.5. Electrocatalytic investigation of UA and Trp

Figure 5 displays the differential pulse voltammograms obtained in the absence and presence of a mixture of UA (65 µM) and Trp (50 µM) in 0.1 M CABS (pH 3.0) at bare GPE (BGPE), NRL/GPE and FCNNRL/GPE modified electrodes. The BGPE showed two weak peak currents for UA and Trp at potential 0.69 and 0.99 V, respectively. The NRL/GPE displayed slightly increasing in the oxidation peak current of UA and Trp in compare of BGPE at potential 0.65 and 0.97 V, respectively. The FCNNRL/GPE displayed a high increasing in the oxidation peak current of UA and Trp in compare of BGPE and NRL/GPE at potential 0.63 and 0.94 V, respectively. It is shown from DPVs at the FCNNRL/GPE that the oxidation peak potential of UA and Trp were shifted by 60 and 50 mV to the negative direction compared in compared to BGPE and 20 and 30 mV with that NRL/GPE for UA and Trp, respectively. Also, the oxidation peak current at FCNNRL/GPE was increased 4.7 and 4.3 times for UA and 3.4 and 1.9 for Trp in compared to GPE and NRL/GPE, respectively. These results showed that FCN into the FCNNRL/GPE had excellent improvement on the electrocatalytic oxidation of UA and Trp and decreasing the over potential of the analytes.

The mechanism of electrocatalytic oxidation of UA and Trp on FCNNRL/GPE surface can be written as follow (EC);

$$2[Fe(CN)_6]^{4-} \longrightarrow 2[Fe(CN)_6]^{3-} + 2e \quad (2)$$

$$2[Fe(CN)_6]^{3-} + UA_{Red} \text{ (or } Trp_{Red}) \longrightarrow 2\,[Fe(CN)_6]^{4-} + UA_{ox} \text{ (or } Trp_{ox}) + 2H^+ \quad (3)$$

The selective determination of UA and Trp at FCNNRL/GPE was studied by the comparison in the simultaneous determination and individual determination of UA and Trp. The results display in Figure 4(B), that indicating the oxidation processes of these two compounds are independent and therefore, simultaneous determination of UA and Trp on FCNNRL/GPE is possible without any significant interferences.

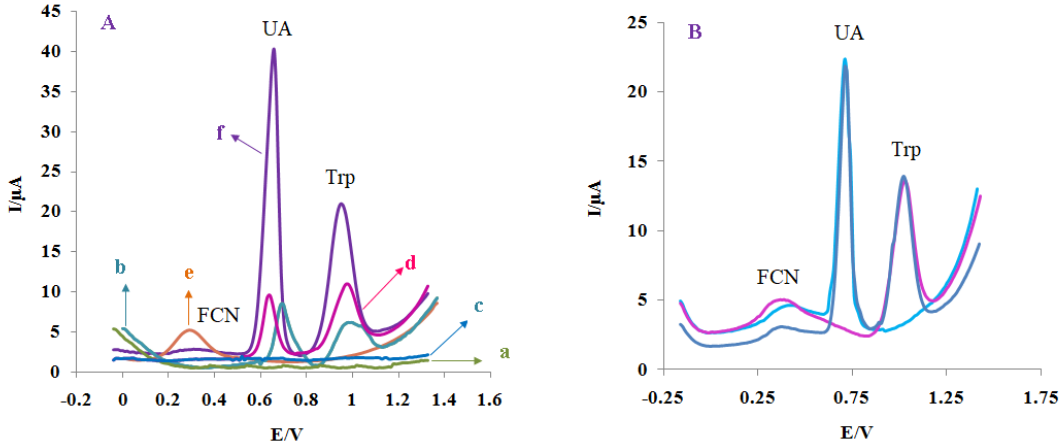

Fig. 5. (A) DPVs of (a) GPE in the absence of UA and Trp, (b) GPE in the presence of UA (65.0) µM and Trp (50.0 µM), (c) NRL/GPE in the absence of UA and Trp, (d) NRL/GPE in the presence of UA (65.0) µM and Trp (50.0 µM) (e) FCNNRL/GPE in the absence of UA and Trp and and (f) FCNNRL/GPE in the presence of UA (65.0) µM and Trp (50.0 µM each) in 0.1 mol.L^{-1} CABS (pH 3.0); (B) *DPV* obtained of comparison the simultaneous determination with single determination of UA (60.0 µM) and Trp (50.0 µM) in 0.1 M CABS with pH 3 at FCNNRL/GPE

3.6. Effect of pH on the oxidation of UA and Try

The effects of pH on anodic peak currents and potentials of UA and Trp on FCNNRL/GPE in the range of 2–5 using 0.1 M CABS were investigated by DPV and the results were shown in Figure 6. Based on Figure, the pH value of electrolyte has an important effect on the electrooxidation of UA and Trp because protons participate in their electrochemical reactions. Figure 6 (b) has been shown that highest peak current was obtained at pH 3 for UA and Trp. In addition, in the selected pH range (2–5), the oxidation peak of potentials of UA and Trp is also pH dependent (see Figure 6(c)) and the E_{pa} of UA

and Trp were shifted to more negative values, with increasing the pH. These results indicate that the protons are directly involved in the electrochemical reaction of the UA and Trp [26,27]. The linear regression equations for variation of the oxidation of UA and Trp *vs.* pH are as follow;

$E_{(pa,\ UA)}$ (V) = 0.860 – 0.0622 pH (r^2 = 0.9836) (4)

$E_{(pa,\ Trp)}$ (V) = 1.130 – 0.0562 pH (r^2 = 0.9878) (5)

These results display that the two lines of E_{pa} vs. *p*H for UA and Trp are almost parallel, which indicates that the difference of the peak potentials was stable in different electrolytes solutions. The observed slopes of 0.0622V/ *p*H and 0.0562V/ *p*H, respectively for UA and Trp are close to the theoretical Nernst value of 0.0591V/pH for two electrons and two protons process [28]. Based on the above results, the probable the electrochemical reaction of UA and Trp at surface of FCNNRL/GPE should be a two- electron and two- proton process (Eqs. 6, 7). Therefore, pH 3.0 CABS was selected as the optimum pH for electrocatalysis of UA and Trp oxidation at the surface of FCNNRL/GPE.

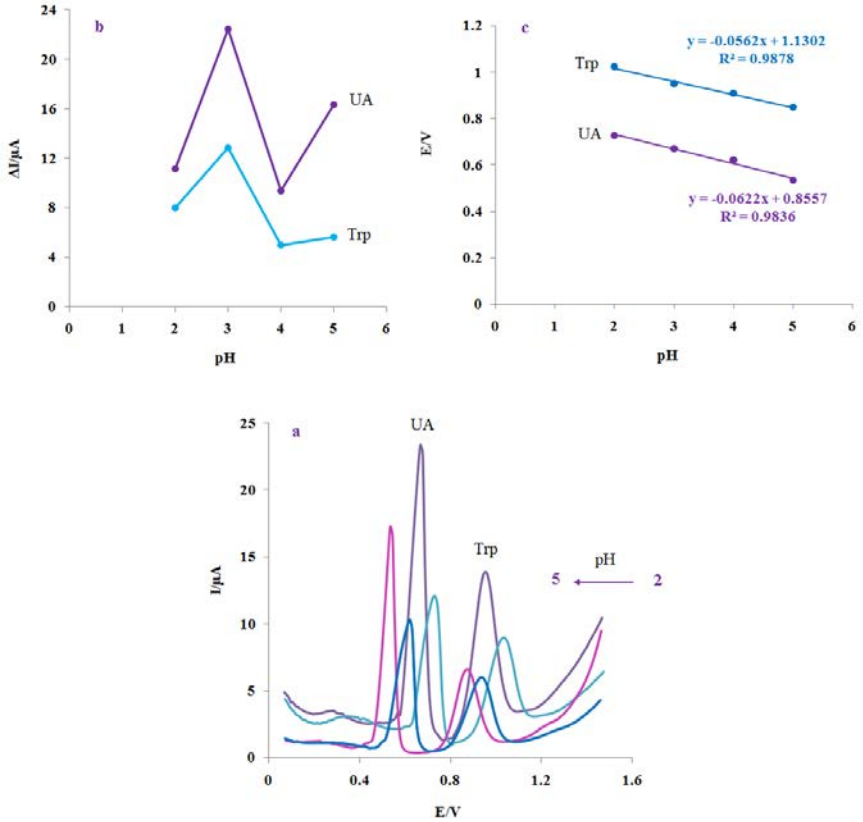

Fig. 6. (a). The effects of pH on the electrocatalytic oxidation of UA (65.0μM each) and Trp (50.0μM each) on FCNNRL/GPE surface in 0.1 mol L^{-1} CABS. (b) Plots of anodic peak currents of UA and Trp vs. pH. (c) Plots of anodic peak potentials of UA and Trp *vs.* pH.

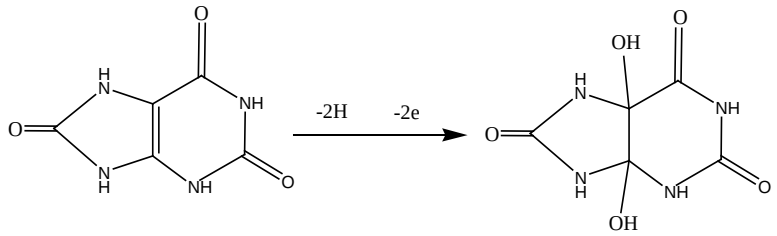

(6)

UA

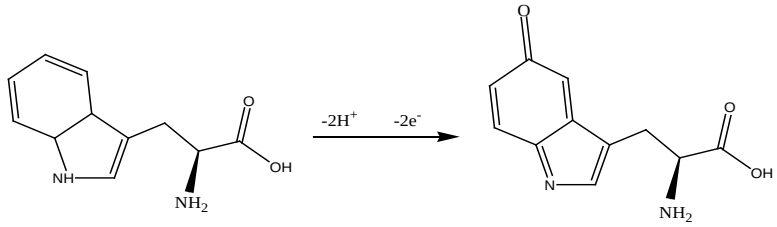

(7)

Trp

3.7. Chronoamperometric studies

Figures 1S, 2S have been shown chronoamperograms obtained for UA and Trp in 0.1 M CABS (pH 3.0) on the FCNNRL/GPE electrode. The plots of I *vs.* $t^{-1/2}$ (Figure 1S, 2S(b)) for different concentrations of UA and Trp gives straight lines which the slopes obtained were then plotted against UA and Trp concentrations, which of the slopes obtained, the diffusion coefficients for UA and Trp were estimated to be according to Cottrell equation (eq. 8) [29], 2.68×10^{-6} and 2.35×10^{-6} cm^2 s^{-1}, respectively.

$$I = nFAD^{1/2}C\pi^{-1/2}t^{-1/2} \quad (8)$$

3.8. Effect of interferences

Possible interference for the detection of UA and Trp on FCNNRL/GPE surface under optimum experimental condition was investigated by increasing the concentration of one species while keeping the concentration of the other species is constant. Figure 3S shows the oxidation peak current of UA increased remarkably with the increase of UA concentration, while the peak current of Trp did not change. As shown in Figure 4S, when the concentration of UA was kept constant, the oxidation peak current of Trp was positively proportional to its concentration. The above results indicate that UA and Trp on FCNNRL/GPE can be separately determined in their mixture using the proposed method.

3.9. Simultaneous detection of UA and Trp

Calibration graph and detection limit for the simultaneous determination of UA and Trp can be evaluated by the DPV method (Figure 7). The plots of oxidation peak current of UA and Trp *vs.* concentration consisted of two linear segments that are because of dependence activity of the FCNNRL/GPE surface to low and high concentration of the analytes. Also,

there are an isopotential point (IPP) in potential 0.54 V that the peak current of FCN decreasing with increasing the concentration of analytes and oxidation peaks currents of UA and Trp. In the lower concentrations of analytes, because of a high number of active sites in relation to the total number of the analyte molecules, the first calibration curve slope for UA and Trp is high. While in the higher concentrations of UA and Trp, because of decreasing active sites in relation to the total number of analyte molecules at FCNNRL/GPE surface, the second calibration curve slope decreased too. The linear relationship exhibited between the peak currents and the concentrations of UA and Trp with two segments in the ranges of 0.4 – 31 and 31-175.2 µM and 0.5-32 and 32-173 µM, respectively. The detection limits were determined to be of 10 and 30 nM for UA and Trp based on $Y_{LOD}= X_{bk} + 3S_{bk}$, where Y_{LOD}, X_{bk} and S_{bk} are signal for detection limit, the mean of blank signal and the standard deviation of the blank signal, respectively.

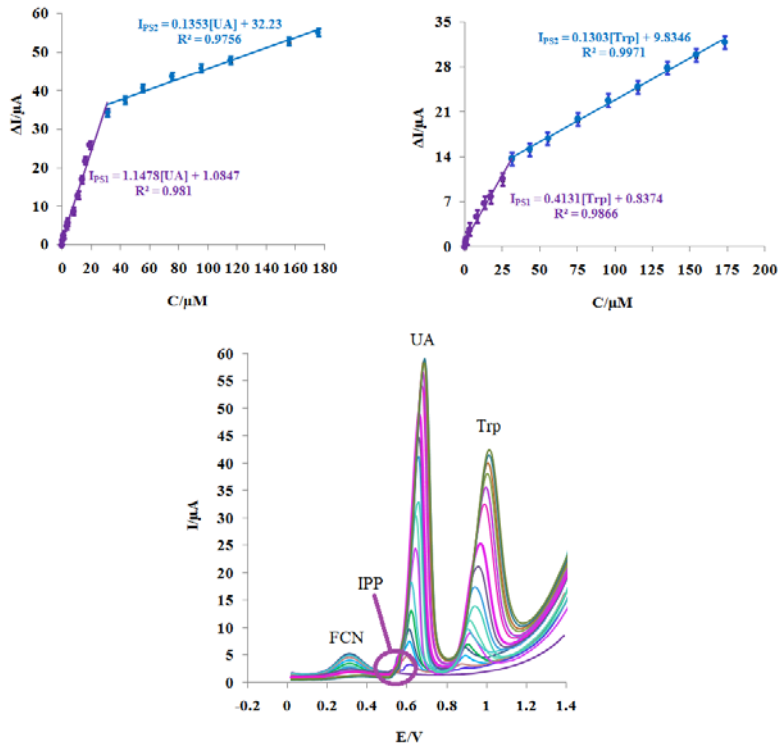

Fig. 7. DPVs of the simultaneous determination of UA and Trp at the FCNNRL/GPE electrode in 0.1 M CABS with pH 3. Concentrations for UA (0.0- 175.2 µM) and Trp (0.0-173.0 µM)

3.12. Determination of UA and Trp in real samples

The proposed FCNNRL/GPE was used to measure the concentrations of UA and Trp in human serum and urine samples. The accuracy of the method in real samples was estimated

by recovery. The recovery of UA and Trp was determined in real samples by spiking UA and Trp standard solutions into the samples before the electrochemical determination by the modified FCNNRL/GPE.

Table 1. Determination of UA and Trp in real samples using FCNNRL/GPE (n=3)

Sample	Analyte	Detected/μM[a]	Added/μM	Found/μM[a]	Recovery/%	RSD/%
Serum 1	UA	0.90±0.04	10.00	9.60±0.04	96.00	0.80
	Trp	ND[b]	22.00	23.20±0.13	105.44	1.54
Serum 2	UA	0.85±0.05	20.00	19.20±0.05	96.00	0.81
	Trp	ND[b]	25.00	24.00±0.20	96.00	2.94
Urine 1	UA	12.60±0.08	22.00	21.30±0.09	96.82	1.55
	Trp	ND[b]	23.00	22.00±0.12	95.65	1.63
Urine 2	UA	10.90±0.14	20.00	19.30±0.16	96.50	2.35
	Trp	ND[b]	24.00	23.70±0.07	98.75	1.20

a. Mean±standard deviation
b. Not detected

Table 2. Comparison the FCNNRL/GPE electrode with other various electroanalytical electrodes for the simultaneous determination of UA and Trp

Electrode	Modifier	Method	pH	Analyte	Linear range/μM	Detection Limit/μM	Ref.
Carbon nanotube paste	N-(3,4-dihydroxyphenethyl)-3,5-dinitrobenzamide	SWV	7.0	UA Trp	5.0 – 420.0 1.0 – 400.0	2.00 0.80	[12]
Carbon fiber microdisk electrode	Electrochemical reduction of graphene oxide	CV	7.4	UA Trp	1.0 – 600.0 0.6 – 600.0	0.6 0.10	[13]
Fluorine-doped-tin oxide electrode	Inorganic ruthenium red dye-multiwalled carbon nanotubes	LSV/CV	3.0	UA Trp	1.3–433.3 1.3–433.3	0.14 0.14	[14]
CPE	multi-walled carbon nanotubes	DPV	3.0	UA Trp	0.4-100.0 0.6-100.0	0.03 0.06	[15]
CPE	pre-anodized inlaying ultra-thin	LSV/CV	5.0	UA Trp	0.5–150 0.1–200	0.04 0.05	[16]
Glassy Carbon	gold nanoparticles (AuNPs) functionalized multiwalled carbon nanotubes	LSV/CV	7.0	UA Trp	1.6– 25.0 1.3 – 50.0	0.6 1.3	[17]
GPE	FCNNRL/GPE	DPV	3.0	UA Trp	0.4-175.2 0.5-173.0	0.01 0.03	This work

The standard addition method was used for analysis of the real samples by the proposed modified electrode. The UA was detected in the serum and urine samples. For simultaneous

determination UA and Trp in serum and urine samples, one mL of serum or urine was added to 10 mL of CABS (0.1 M, pH 3.0) in electrochemical cell. After each addition of UA and Trp standard solutions DPVs were recorded and the results obtained for spikes of these electroactive compounds to real samples are summarized in Table 1. The recovery was obtained between 95.6 and 105.4% which indicate FCNNRL/GPE can be successfully applied to the determination of UA and Trp with good accuracy in real samples.

4. CONCLOSION

In this research, for the first time a novel FCNNRL/GPE was prepared and applied for simultaneous determination of UA and Trp. This modified electrode was characterized by CV, ESI, TEM and FT-IR techniques. The CV and DPV investigations displayed excellent electrocatalytic activity of the FCNNRL/GPE in lowest anodic over potential and highest peak currents for the electrooxidation of UA and Trp. High sensitivity, long time stability, selectivity, cheap, well anti-interference ability, good reproducibility of the voltammetric responses, reliability, fast response for the detection of UA and Trp, wide linear range and very low detection limit are the advantages of this modified electrode. The figures of merit of proposed electrode were compared with literature in Table 2. Based on this table, the figures of merit of the proposed modified electrode such as modifiers, linear range and detection limit were compared for the determination of the UA and Trp with some reported works. In the some cases, the proposed sensor shows a good linear range and lower detection limit and in other cases shows satisfactory results in comparison to other literatures. So, the proposed modified electrode is a good candidate for simultaneous determination of UA and Trp with satisfactory results in comparison with the other literatures. Finally, the FCNNRL/GPE was applied for simultaneous determination of UA and Trp in real samples, with excellent results.

REFERENCES

[1] S. Thiagarajan, and S. M. Chen, Talanta 74 (2007) 212.
[2] X. Tang, Y. Liu, H. Hou, and T. You. Talanta 80 (2010) 2182.
[3] Y. Zhu, Y. Yang, Z. Zhou, G. Li, M. Jiang, C. Zhang, and S. Chen, Food Chem. 118 (2010) 159.
[4] S. Hanaoka, J. Lin, and M. Yamada, Anal. Chim. Acta 409 (2000) 65.
[5] J. Zhao, Biomedical Chromatography 29 (2015) 410.
[6] C. G. Honegger, W. Krenger, H. Langemann, and A. Kempf, J. Chromatogr. B 381 (1986) 249.
[7] W. Jin, X. Li, and N. Gao, Anal. Chem. 75 (2003) 3859.
[8] S. Zhao, J. Wang, F. Ye, and Y. M. Liu, Anal. Biochem. 378 (2008) 127.
[9] J. C. Fanguy, and C. S. Henry, Electrophoresis 23 (2002) 767.

[10] S. Chen, H. Zheng, J. Wang, J. Hou, Q. He, H. Liu, C. Xiong, X. Kong, and Z. Nie, Anal. Chem. 85 (2013) 6646.
[11] M. I. Evgen'ev, and I. I. Evgen'eva, J. Anal. Chem. 55 (2000) 741.
[12] H. S. Yin, Q. M. Zhang, Y. L. Zhou, Q. A. Ma, T. Liu, L. S. Zhu, and S. Y. Ai, Electrochim. Acta 56 (2011) 2748.
[13] B. Kaur, T. Pandiyan, B. Satpati, and R. Srivastava, Coll. Surfaces B 111 (2013) 97.
[14] Q. Lian, Z. He, Q. He, A. Luo, K. Yan, D. Zhang, X. Lu, and X. Zhou, Anal. Chim. Acta 823 (2014) 32.
[15] L. Cumbal, A. K. Sengupta, Environ. Sci. Technol., 39 (2005) 6508.
[16] I. Švancara, K. Vytřas, J. Barek, and J. Zima, Anal. Chem. 31 (2011) 311-345.
[17] J. F. Duncan, and P. W. R. Wrigley, J. Chem. Soc. (1963) 1120.
[18] M. Noroozifar, M. Khorasani-Motlagh, and P. Ahmadzadeh Fard, Hazard. Mater. 166 (2009) 1060.
[19] J. G. Manjunatha, M. Deraman, N. H. Basri, N. S. Mohd Nor, I. A. Talib, and N. Ataollahi, Comptes. Rendus. Chim. 17 (2014) 465.
[20] M. Sharp, M. Petersson, and K. Edstrom, Electroanal. Chem. 95 (1979) 123.
[21] S. K. Hassaninejad–Darzi, and M. Rahimnejad, J. Iranian Chem. Soc. 11 (2014) 1047.
[22] H. Gharibi, K. Kakaei, and M. Zhiani, Phys. Chem. 114 (2010) 5233.
[23] Z. Liu, Z. Wang, Y. Cao, Y. Jing, and Y. Liu, Sens. Actuators B 157 (2011) 540.
[24] Q. Guo, J. Huang, P. Chen, Y. Liu, H. Hou, and T. You, Sens. Actuators B 163 (2012) 179.
[25] S. H. DuVall, R. L. McCreery, Anal. Chem. 71 (1999) 4594.
[26] Q. Guo, J. Huang, P. Chen, Y. Liu, H. Hou, and T. You, Sens. Actuators B 163 (2012) 179.